

Practical and Theoretical Study on the α -Substituent Effect on α -Diimine Nickel(II) and Cobalt(II)-Based Catalysts for Polymerization of Ethylene¹

Mostafa Khoshsefat^a, Narges Beheshti^b, Gholam Hossein Zohuri^{b,*},
Saeid Ahmadjo^a, and Somaye Soleimanzadegan^b

^aDepartment of Catalyst, Iran Polymer and Petrochemical Institute, Tehran, Iran

^bDepartment of Chemistry, Faculty of Science, Ferdowsi University of Mashhad, Mashhad, Iran

*e-mail: zohuri@um.ac.ir

Received January 26, 2016; Revised Manuscript Received May 1, 2016

Abstract—The Late transition metal catalysts based on Ni(II) and Co(II) were synthesized and their structure and activity in polymerization of ethylene were compared. Methylaluminoxane (MAO) was used as a co-catalyst. To discover the optimum polymerization conditions, the effect of polymerization temperature, monomer pressure, [Al] : [Ni] molar ratio and time of polymerization were studied. Activity of the catalysts was promoted by increasing of the monomer pressure. The viscosity average molecular weights M_v of the synthesized polymers using 1,2-bis(2,4,6-trimethyl phenyl imino) acenaphthene Nickel(II) dibromide were increased with increasing of the monomer pressure from 1 up to 6 bar which studied. Explicitly, the ortho-substituent has a significant effect on the catalyst behavior. Melting point and crystallinity of the obtained polyethylene using 1,2-bis(2,4,6-trimethyl phenyl imino) acenaphthene Nickel(II) dibromide catalyst were increased with enhancing monomer pressure. The optimum and stable structures were computed and some factors related to the activity were studied. Catalyst 1,2-bis(2,4,6-trimethyl phenyl imino) acenaphthene Nickel(II) dibromide had the highest activity with the highest quantities of dipole moment (18.29 Debye), charge of Mullikan on metal atom (1.48) and Sum of electronic and thermal Energies (−7906.52 e.u.).

DOI: 10.1134/S1560090416050067

INTRODUCTION

Transition metal catalysis for polymerization of olefins are vital to the plastic industry [1], which are manufactured employing Ziegler–Natta, metallocene and Philips catalysts [2–4]. In addition to metallocene catalysts, another major advancement in the area of olefin polymerization was the discovery of the homogeneous α -diimine based late transition metal catalysts (Ni and Pd) in 1995 [5]. Early transition metals, which are applied in polyolefins synthesis are based on Ti, Zr, Cr, and V. These catalysts have oxophilic property, and this lead to be

reactive toward water and oxygen [6–10]. The late transition metals (Ru, Co, Rh, Ni, and Pd), however, are much less oxophilic and therefore they may be used even in aqueous systems [11–13]. The late transition metal catalysts systems, therefore, are able to produce highly branched and low molecular weight polymers of ethylene [14].

The first synthesis of branched polyethylene solely from ethylene monomer using a nickel catalyst was reported in 1981 by W. Keim and co-workers, 14 years prior to disclosure of practical catalysts based on Ni α -diimine complexes [15]. The nickel α -diimine complexes represent an attractive group of such catalysts due to their high polymerization activity [16], lower oxophilicity, easy synthesis and

¹ The article is published in the original.

the fact that they do not need high Al/metal ratios for catalyst activation [17]. Many articles discuss the influence of variables such as polymerization temperature, monomer pressure, catalyst structure and role of bulky substituents on polymerization using α -diimine Ni(II) catalysts [18–20].

The activities and selectivity to reach α -olefins are dependent on the catalyst structure. The steric bulk groups around the metal center of the catalysts are a key to retarding chain transfer reaction to obtain high molecular weight polyethylene. The protective bulky groups of the ortho-substituents above and below the metal active centers was critical to the molecular weight of the resulting ethylene polymerizations [17, 21–23]. There are many striking papers and reviews on the late transition metal, especially on α -diimine Nickel catalysts, which have been published [14, 17, 22–29].

In this work six catalysts, namely Ni(II)- and Co(II)-based late transition metal complexes, were synthesized and characterized. Each group of complexes differs in the methyl substituent positions. The ortho-substituent effect on the catalyst performance in ethylene polymerization was investigated. Moreover, optimization of polymerization condition and comparison between catalysts both practically and theoretical factors related to the catalyst activity were the aims of this work.

EXPERIMENTAL

Materials and Polymer Synthesis

All manipulations of air and/or water sensitive compounds were conducted under argon/nitrogen atmosphere using the standard Schlenk techniques. All the solvents were purified prior to use. Toluene (purity 99.9%) (Iran, Petrochemical Co.) was purified over sodium wire/benzophenone, and used as polymerization solvent. Dichloromethane (purity 96%) (Sigma Aldrich Chemicals, Germany) was purified over calcium hydride powder, and distilled prior to use as a complex synthesis solvent. Polymerization grade ethylene gas (purity 99.9%) (Iran, Petrochemical Co.) was purified by passing through activated silica gel, KOH, and 4 Å/13 X molecular sieves column. 2,4,6-trimethylaniline, 2,3-dimethylaniline, 3-methylaniline,

acenaphthoquinon, Cobalt(II) chloride, Nickel(II) bromide ethylene glycol dimethyl ether complex [(DME)NiBr₂] (purity 97%) and diethyl ether (purity 99.5%) were supplied by Merck Chemical (Darmstadt, Germany) and used in synthesis of ligands and catalysts. Decaline (decahydronaphthalene) (purity 97%) was purchased from Sigma Aldrich Chemicals (Steinheim, Germany). Triisobutylaluminium (purity 93%) (TIBA) was supplied by Sigma Aldrich Chemicals (Steinheim, Germany) which was used in synthesis of methylaluminumoxane (MAO) according to the literature [30].

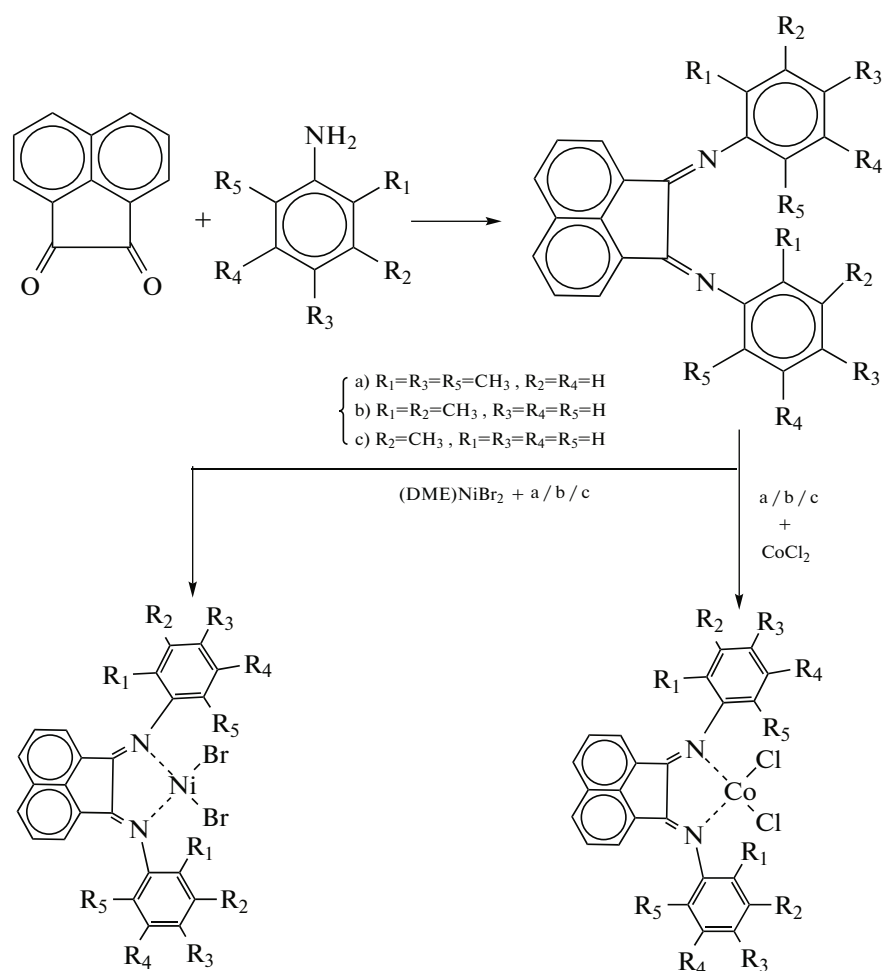
Two kind of polymerization in low and high pressure were employed. The low pressure process was carried out in a 100 mL round bottom flask which was equipped with Schlenk system, vacuum line, ethylene inlet and magnetic stirrer. The high pressure (more than 2 bar) was carried out using a 1 L Buchi bmd-300 type reactor.

Characterization

¹H NMR and FTIR spectrums were obtained using Bruker AC-80 and Bruker IF-505 spectrometers, respectively. Elemental analysis was performed on a Thermo Finnigan Flash 1112EA microanalyzer. The viscosity average molecular weight M_v of some polymer samples was determined according to the literature [31]. Intrinsic viscosity η was measured in decaline at $133 \pm 1^\circ\text{C}$ using an Ubbelohde viscometer. M_v values were calculated through Mark-Houwink $[\eta] = KM_v^\alpha$ equation ($\alpha = 0.7$, $K = 6.2 \times 10^{-4}$) [20]. Differential scanning calorimetry (DSC) (Q100 Perkin Elmer) with a rate of 10 grad/min instrument was used for polymer characterization.

Synthesis of Ligands and Complexes

The general reaction for synthesis of the ligands and catalysts are shown in Scheme.



Scheme 1.

Ligand a. 2,4,6-Trimethyl aniline (7 mmol) was added to a stirred solution of acenaphthoquinone (0.5 g, 3 mmol) in methanol (15 mL) and in the presence of catalytic amount of formic acid. The solution was stirred for 48 h. Progress of the reaction was checked by TLC. The solvent was evaporated at the end of the reaction and the precipitate was washed with *n*-hexane and recrystallized using ethanol (brown solid). Yield: 89%. ¹H NMR (CDCl₃, 100 MHz) δ_H, ppm: 2/2 (s, 12H), 2/35 (s, 6H), 7 (s, 4H), 6/8 (d, 2H), 7/4 (q, 2H), 8 (d, 2H). FTIR (KBr, cm⁻¹): 1647 (–C=N–), 1234 (–C–N–). Anal. Calc. for C₃₀H₂₈N₂, %: C, 86.5; H, 6.7; N, 6.7 Found, %: C, 86.7; H, 6.5; N, 6.6.

Ligand b. The α-diimine ligand preparation was carried out according to the method described above but instead of 2,4,6 trimethyl aniline, 2,3 dimethyl aniline was used. The ligand was obtained as brown solid. Yield: 94%. ¹H NMR (CDCl₃, 100 MHz) δ_H, ppm: 2/1 (s, 6H), 2/35 (s, 6H), 6/8–7 (m, 4H), 7/2 (d, 2H), 7/5 (d, 2H), 7/85–8 (m, 4H). FTIR (KBr, cm⁻¹): 1655 (–C=N–), 1274 (–C–N–). Anal. Calc. for C₂₈H₂₄N₂, %: C, 86.6; H, 6.2; N, 7.2. Found, %: C, 86.5; H, 6.1; N, 7.3.

Ligand c. The α-diimine ligand preparation was carried out similarly but instead of 2,4,6-trimethyl aniline, 3-methyl aniline was used. The ligand was obtained as brownish solid. Yield: 98%. ¹H NMR (CDCl₃, 100 MHz) δ_H, ppm: 2/3 (s, 6H), 6/8–7/1 (m, 6H), 7/3–7/5 (m, 6H), 8 (d, 2H). FTIR (KBr, cm⁻¹): 1650 (–C=N–), 1282 (–C–N–). Anal. Calc. for C₂₆H₂₀N₂, %: C, 86.6; H, 5.6; N, 7.8. Found, %: C, 86.7; H, 5.5; N, 7.7.

Synthesis of complex A₁. Nickel(II) bromide ethylene glycol dimethyl ether complex (DME)NiBr₂ (0.074 g, 0.24 mmol) and solution of ligand a (0.1 g, 0.24 mmol) in 15 mL dichloromethane were combined under atmosphere of nitrogen to prepare Ni-based α-diimine catalyst A₁ (Scheme 1). The solution was stirred at room temperature for 24 h. The solvent was removed and the residual solid was purified and washed with diethyl ether. FTIR (KBr, cm⁻¹): the imine signal was shifted to weak field as it coordinated to the Ni; 1622 (–C=N–). Anal. Calc. for C₃₀H₂₈Br₂N₂Ni, %: C, 56.7; H, 4.4; N, 4.4. Found, %: C, 57.2; H, 5.0; N, 4.7.

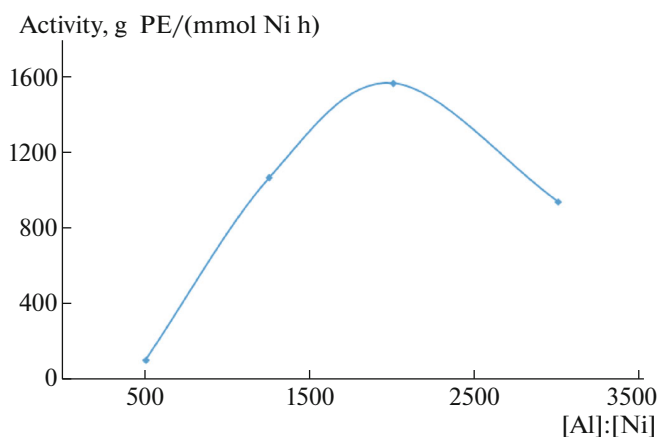


Fig. 1. (Color online) Effects of the [Al] : [Ni] molar ratio on the activity of catalyst A_1 . Condition: temperature 30°C, monomer pressure 1 bar, polymerization time 30 min, toluene 35 mL, catalyst 3.15×10^{-3} mmol.

Synthesis of complex B_1 . This compound was prepared using a similar procedure with the exception that ligand b was used. FTIR (KBr, cm^{-1}): the imine signal was shifted to weak field as it coordinated to the Ni; 1625 ($-\text{C}=\text{N}-$). Anal. Calc. for $\text{C}_{28}\text{H}_{24}\text{Br}_2\text{N}_2\text{Ni}$, %: C, 55.4; H, 4.0; N, 4.6. Found, %: C, 56.5; H, 4.2; N, 4.4.

Synthesis of complex C_1 . This compound was prepared using a similar procedure applying ligand c. FTIR (KBr, cm^{-1}): the imine signal was shifted to weak field as it coordinated to the Ni; 1638 ($-\text{C}=\text{N}-$). Anal. Calc. for $\text{C}_{26}\text{H}_{20}\text{Br}_2\text{N}_2\text{Ni}$, %: C, 53.9; H, 3.5; N, 4.8. Found, %: C, 54.6; H, 4.8; N, 4.2.

Synthesis of complex A_2 . Cobalt(II) chloride (0.16 g, 1.2 mmol) and dichloromethane (20 mL) were combined and stirred. A red solution of ligand a (0.5 g, 1.2 mmol) in 10 mL dichloromethane was added to the first blue compound. The solution was stirred for 24 h to dissolve completely. Through a partially removing solvent, a red-brown solid appeared. After filtration, the solid was washed by petroleum ether for two times and then purified. FTIR (KBr, cm^{-1}): the imine signal was shifted to weak field as it coordinated to the Co; 1628 ($-\text{C}=\text{N}-$). Anal. Calc. for $\text{C}_{30}\text{H}_{28}\text{Cl}_2\text{CoN}_2$, %: C, 66.0; H, 5.2; N, 5.1. Found, %: C, 64.9; H, 5.1; N, 4.5.

Synthesis of complex B_2 . This complex was prepared using a similar procedure as for A_2 but applying ligand b. FTIR (KBr, cm^{-1}): the imine signal was shifted to weak field as it coordinated to the Co; 1634 ($-\text{C}=\text{N}-$). Anal. Calc. for $\text{C}_{28}\text{H}_{24}\text{Cl}_2\text{CoN}_2$, %: C, 64.9; H, 4.7; N, 5.4. Found, %: C, 64.8; H, 4.5; N, 5.3.

Synthesis of complex C_2 . This compound was prepared using a similar procedure as for A_1 with the

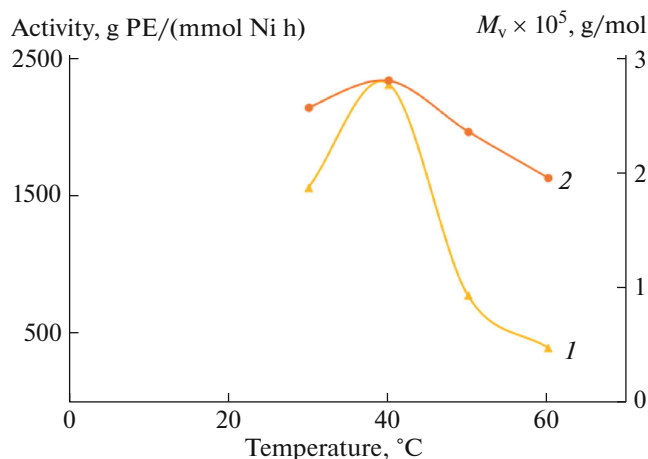


Fig. 2. (Color online) Effects of temperature on (1) the activity of catalyst A_1 and (2) M_v . Condition: monomer pressure 1 bar, polymerization time 30 min, toluene 35 mL, [Al] : [Ni] = 2000, catalyst 3.15×10^{-3} mmol.

exception that ligand c replaced. FTIR (KBr, cm^{-1}): the imine signal was shifted to weak field as it coordinated to the Co; 1643 ($-\text{C}=\text{N}-$). Anal. Calc. for $\text{C}_{26}\text{H}_{20}\text{Cl}_2\text{CoN}$, %: C, 63.7; H, 4.1; N, 5.7. Found, %: C, 63.2; H, 4.5; N, 5.8.

RESULTS AND DISCUSSION

In order to achieve the maximum activity of the polymerization, the catalyst A_1 (3.15×10^{-3} mmol) was used. The polymerization was performed under constant pressure (1 bar) and the temperature (30°C) for 30 min. Following to addition of MAO, a change in color from brown into purple occurred probably due to generation of a new coordination site and ligand substitution.

The effect of the molar ratio of [Al] : [Ni] on the polymerization behavior was studied in the range of 500 up to 3000. The optimum activity was achieved at [Al] : [Ni] molar ratio of 2000 : 1 (Fig. 1). The activity was decreased gradually because of MAOz witter ion formation and the active species of catalyst that evinced the increase of reverse reaction rate and formation of inactive complex [32, 33].

To study the effect of the polymerization temperature and to discover the optimum temperature and also the effect on the viscosity average molecular weight M_v , the experiments were carried out under constant monomer pressure (1 bar), [Al] : [Ni] molar ratio (2000 : 1), time (30 min) and various temperatures in the range of 30 to 60°C. The results are depicted in the Fig. 2. By considering the obtained results, the best temperature for achieving the most resulting polymer with the highest M_v and the activity is 40°C. Before taking to the optimum temperature, at lower polymerization temperature, rate determined

Table 1. Ethylene polymerization using A_1 catalyst

Run	Pressure, bar	Activity, g PE/(mmol Ni h)	M_v	ΔH_{melt} , Cal/g	Crystallinity, %	Melting point, °C
1	1	1563	2.57×10^5	98	—	117, 131
2	3	2344	3.19×10^5	31	51	104
3	5	2694	3.61×10^5	79	—	129, 137
4	6	5188	4.26×10^5	43	71	131

*Condition: polymerization temperature 30°C, polymerization time 30 min, toluene 200 mL, [Al] : [Ni] = 2000 : 1, catalyst 3.15×10^{-3} mmol.

state is transfer and adsorption monomer to active center and with increasing the polymerization temperature, possibility of aiming monomer to the active centers increases and the required activation energy for propagation of polymer provides [34]. Thus, increase of the polymerization temperature facilitates the rates of active center formation, alkylation, and finally results in higher yield of the polymer.

In contrast, decaying of active centers (chemical factor) and the decreasing solubility of monomer (physical factor) in reaction media at higher temperature cause the activity of the catalyst to decrease [34, 35].

To study the effect of polymerization pressure, the experiments were carried out under constant temperature (30°C), [Al] : [Ni] molar ratio (2000 : 1), polymerization time (30 min) and various monomer pressure from 1 up to 6 bar. The results are shown in the Table 1 and Fig. 3. Increasing of the pressure causes rise of the monomer concentration in polymerization media and prevents chain transfer reactions. In addition, polymerization rate is directly proportional to monomer pressure. For these reasons, activities and the viscosity average molecular weights of the polymer produced

increased. The non-linear relationship between monomer pressure and activity is fully described in the literature [36–38]. The thermal behaviors of polymer produced using catalyst A_1 are reported in Table 1. Increasing of side chains density leads to decreasing of crystallinity and melting point of the polymer produced, consequently (Table 1). At low ethylene pressure, chain migration is not interrupted by trapping by ethylene, allowing the metal to migrate large distances between insertions. However, the higher is the monomer pressure, the less is chain transfer, which caused formation of linear polymer with relatively short branches. In addition, the broadening transition commonly has been attributed to a sequence of melting followed by recrystallization steps of less ordered domains with the variable amounts of short-chain branching as a function of molecular weight that similar behaviors previously were report [37, 39, 40].

Polymerization activity was increased to an optimum value after about 10 min of the reaction. The behavior may refer to being alkylated all active centers by co-catalyst and the availability of monomers. In contrast, decreasing in mass diffusion causes more side reactions such as transfer to monomer and β -hydride elimination and decreasing of propagation

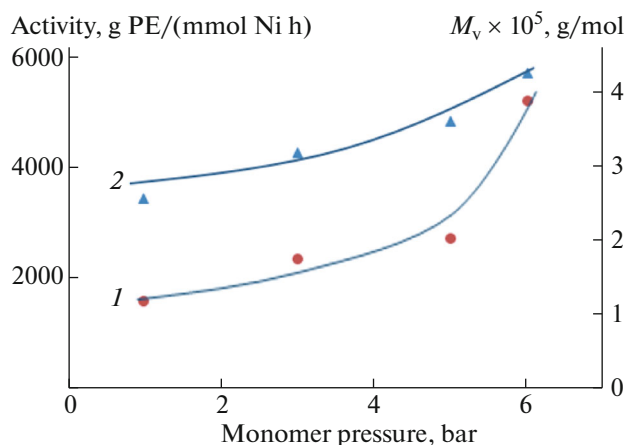


Fig. 3. (Color online) Effects of monomer pressure on (1) the activity of catalyst A_1 and (2) M_v of the polymer obtained.

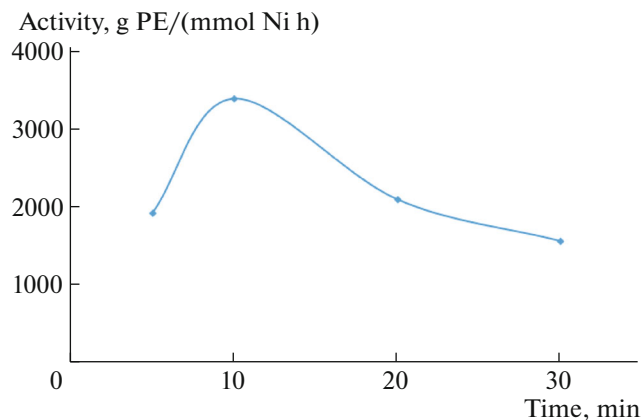


Fig. 4. (Color online) Effects of polymerization time on activity of catalyst A_1 . Condition: temperature 30°C, monomer pressure 1 bar, toluene 35 mL, [Al] : [Ni] = 2000 : 1, catalyst 3.15×10^{-3} mmol.

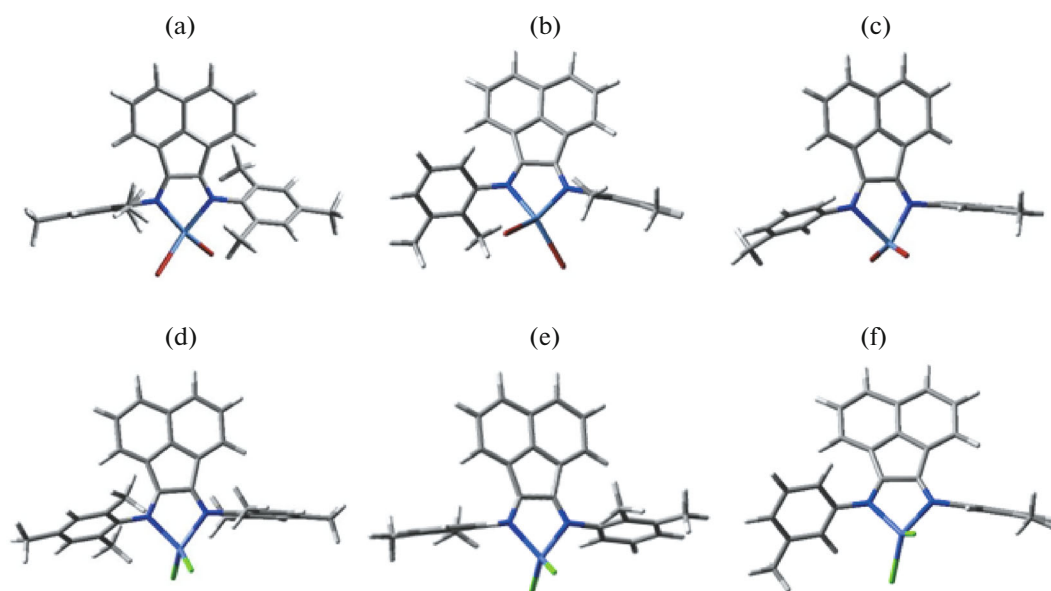


Fig. 5. (Color online) The optimized structure of the complexes: (a) A_1 , (b) B_1 , (c) C_1 , (d) A_2 , (e) B_2 , and (f) C_2 .

reactions, consequently. Also, possibility of irreversible decaying of catalyst active centers increases by polymerization time [10, 20, 41]. The results are illustrated in Fig. 4.

Table 2. Ethylene polymerization using B_1 , C_1 , A_2 , B_2 and C_2 catalysts

Run	Catalysts	[Al]/[M]	T , °C	Activity $\times 10^3$, g PE/(mmol M h)
1	B_1	2000	10	1250
2	B_1	2000	20	12500
3	B_1	2000	30	8750
4	B_1	2000	40	6250
5	B_1	1250	20	6250
6	B_1	500	20	3750
7	C_1	2000	30	2500
8	C_1	2000	15	10000
9	C_1	2000	20	7500
10	C_1	1250	15	6250
11	C_1	500	15	1250
12	A_2	500	20	200
13	A_2	500	40	160
14	A_2	1000	20	1000
15	A_2	2000	20	400
16	B_2	1000	20	200
17	C_2	1000	20	0

B_1, C_1 ; [M] = [Ni], A_2, B_2, C_2 ; [M] = [Co].

Condition: monomer pressure 2 bar, polymerization time 30 min, toluene 35 mL, catalyst B_1, C_1 0.016 mmol, A_2, B_2, C_2 0.01 mmol.

Polymerization of ethylene using catalyst B_1 shows the optimum temperature for the reaction in 20°C. Polymerization activity increased as increasing [Al] : [Ni] molar ratio to 2000 : 1. The highest activity for the catalyst C_1 was observed at same molar ratio but in polymerization temperature of 15°C (Table 2). Similar behaviors were observed for Co(II)-based catalysts. In order to compare the activity of the catalysts, polymerization was implemented in the same conditions. Co(II)-based catalysts, generally, have lower activity than Ni(II)-based. Catalyst A_2 which have substituent (methyl) groups on ortho position of phenyl rings had the highest activity than catalyst B_2 and C_2 . Indeed, this issue due to the structure and electronic effect of ligands and the metal atoms of catalysts. To clarify, α -substituent effect of ligands shows itself on side reaction (transfer to monomer and β -hydride elimination).

To study the structures and role of bulky substituents on the catalysts behavior, some theoretical parameters of catalysts were calculated that are useful to predict the best and the most stable configuration of them. Density Functional Theory (DFT) was used to build the structure and calculate those parameters in the gas phase by using Becke-Lee-Yange-Parr (B3LYP) function. These factors can be related to activity of catalysts such as the dipole moment, electronic energy, band gap and Mullikan charge on the metal atom [41–43].

Optimized structures of catalysts are illustrated in Fig. 5 and the results are listed in the Table 3. Based on the study, angles of X-M-X bonds are 102.1°, 122.7° and 151.9° for A_1, B_1 and C_1 complexes, respectively. Also, for Co(II)-based complexes, it shows an increasing amount of the angle due to absence of ortho-sub-

Table 3. Bond distances (Å), bonds angles (deg) and some physical properties for the optimized structure of the complexes

	A ₁	B ₁	C ₁	A ₂	B ₂	C ₂
M–X	2.42	2.42	2.39	2.38	2.37	2.37
M–N	2.04	2.04	2.35	2.07	2.01	2.01
C=N	1.27	1.27	1.26	1.27	1.26	1.26
X–M–X	102.10	104.35	151.9	123.11	127.41	154.56
M–N–C(phenyl)	123.77	122.7	127.3	125.86	125.88	123.48
M–N–C*	128.60	83.30	112.2	120.20	124.15	105.89
P ₁ –P ₂	40.42	54.30	21.12	0.27	14.82	58.01
Dipole moment (Debye)	18.29	17.53	12.46	16.82	16.82	16.12
Band gap, eV	0.30	0.31	0.34	0.34	0.35	0.35
Charge of Mullikan on M	1.48	1.30	1.27	1.60	1.38	1.37
Sum of electronic and thermal energies, e.u.	–7906.52	–7828.53	–7750.55	–3560.49	–3465.57	–3388.01

C*: Carbon belong to phenyl ring on the α -position.

P₁ and P₂: planes of the two phenyl rings.

stituent (methyl) allowing the bonds to scratch and use all spaces to go far from each other. Dipole moment, band gap, charge of Mullikan on Metal and electronic energy are parameters which can be affected on the catalyst behavior. Based on the table and structures, with increasing in electronic effects around the metal atom of the complex, activity of catalyst in producing polyethylene increased.

CONCLUSIONS

α -Diimine catalysts based on Nickel (A₁, B₁, and C₁) are more active than cobalt based (A₂, B₂, and C₂), and among these, catalyst A₁ had the highest activity. On structure dependence, catalyst B₁ and B₂ are more active than C₁ and C₂, respectively, because of more hindered substituents on aryl rings. With increasing hindering especially on ortho-position of aryl rings, β -hydrogen elimination and chain transfer are retarded due to reduction of monomer diffusion from ortho-position to metallic center. Thus it enhances the viscosity average molecular weight of the polymer produced. Every parameter like temperature, [Al] : [Ni] molar ratio and monomer pressure has an optimum quantity (for Ni(II) based catalysts) which is stated. Catalyst A₁ in comparison catalysts B₁ to C₂ had the highest activity with the highest quantities of dipole moment (18.29 Debye), charge of Mullikan on metal atom (1.48) and Sum of electronic and thermal Energies (–7906.52 e.u.). These factors showed a relation between activity and electronic effects of bulky ligands of complexes. To summarize, not only does activity depends on structures and substituents, but also there is an optimum condition for each catalyst.

ACKNOWLEDGMENTS

We are grateful of Iran Polymer and Petrochemical Institute for all their cooperation.

REFERENCES

1. T. J. Pullukat and R. E. Patterson, in *Handbook of Transitional Metal Polymerization Catalysts* (Wiley, New Jersey, 2010).
2. T. E. Nowlin, R. I. Mink, and Y. V. Kissin, in *Handbook of Transitional Metal Polymerization Catalysts* (Wiley, New Jersey, 2010).
3. L. Wu and S. E. Wanke, in *Handbook of Transitional Metal Polymerization Catalysts* (Wiley, New Jersey, 2010).
4. M. P. McDaniel, in *Handbook of Transitional Metal Polymerization Catalysts* (Wiley, New Jersey, 2010).
5. L. K. Johnston, C. M. Killian, and M. Brookhart, *J. Am. Chem. Soc.* **117** (23), 6414 (1995).
6. W. Kaminsky, *J. Polym. Sci., Part A: Polym. Chem.* **42**, 3911(2004).
7. W. E. Piers and T. Chivers, *Chem. Soc. Rev.* **26**, 345(1997).
8. Sh. Matsui and T. Fujita, *Catal. Today* **66**, 63(2001).
9. J. Huang, B. Lian, Y. Qian, and W. Zhou, *Macromolecules* **35**, 4871 (2002).
10. G. H. Zohuri, S. Damavandi, S. Ahmadjo, R. Sandaroods, and A. M. Shamekhi, *Polyolefins J.* **1**, 25(2014).
11. S. N. Sauca and J. M. Asua, *Chem. Eng. J.* **168**, 1319(2011).
12. L. Wang and Q. Wu, *Eur. Polym. J.* **43**, 3970(2007).
13. B. R. James and L. D. Markham, *J. Catal.* **27**, 442(1972).
14. G. W. Son, K. B. Bijal, D. W. Park, Ch. S. Ha, and I. Kim, *Catal. Today* **111**, 412 (2006).
15. S. Collins, in *Handbook of Transitional Metal Polymerization Catalysts* (Wiley, New Jersey, 2010).

16. H. Pourtaghi-Zahed and G. H. Zohuri, *J. Polym. Res.* **19**, 9996 (2012).
17. J. Merna, Z. Hostalek, J. Peleska, and J. Roda, *Polym. J.* **50**, 5016 (2009).
18. J. P. L. Santos, M. Castier, and P. A. Melo, *Polym. J.* **48**, 5152 (2007).
19. M. Delferro and T. J. Marks, *Chem. Rev.* **111** (3), 2474 (2011).
20. S. Damavandi, N. Samadieh, S. Ahmadjo, Z. Etemadinia, and G. H. Zohuri, *Eur. Polym. J.* **64**, 118(2015).
21. G. J. P. Britovsek, S. P. D. Baugh, O. Hoarau, V. C. Gibson, D. F. Wass, A. J. P. White, and D. J. Williams, *Inorg. Chim. Acta.* **345**, 279(2003).
22. I. Kim, B. H. Han, Y. S. Ha, Ch. S. Ha, and D. W. Park, *Catal. Today* **93**, 281 (2004).
23. L. K. Johnson, S. Mecking, and M. Brookhart, *J. Am. Chem. Soc.* **118**, 267 (1996).
24. H. Zou, F. M. Zhu, Q. Wu, J. Y. Ai, Sh. and A. Lin, *J. Polym. Sci., Part A: Polym. Chem.* **43**, 1325 (2005).
25. H. Zou, Sh. Hu, H. Huang, F. Zhu, and Q. Wu, *Eur. Polym. J.* **43**, 3882 (2007).
26. M. Jeon, Ch. J. Han, and S. Y. Kim, *Macromol. Res.* **14**(3), 306 (2006).
27. J. Long, H. Gao, F. Liu, K. Song, L. Zhang, F. Zhu, Q. Wu, and H. Hu, *Inorg. Chim. Acta.* **362**, 3035(2009).
28. H. Liu, W. Sun, and W. Zhang, *WO Patent No.* 2012122854 A1 (2012).
29. L. Li, M. Jeon, and S. Y. Kim, *J. Mol. Catal. A: Chem.* **303**, 110 (2009).
30. S. A. Sangokoya, *EP Patent No.* 0463555 B1 (1996).
31. J. Brandrup and E. H. Immergut, *Polymer Handbook* (Wiley, New York, 1989).
32. L. Wang and J. Sun, *Inorg. Chim. Acta.* **361**, 1843 (2008).
33. K. P. Bryliakov, E. P. Talsi, and M. Bochmann, *Organometallics* **23**, 149 (2004).
34. G. H. Zohuri, S. Ahmadjo, S. Damavandi, and R. Sandaroos, *Polym. Bull.* **66**, 1051 (2011).
35. E. N. Jacobson and R. Breinbauer, *Science* **287**, 437 (2000).
36. G. H. Zohuri, S. Damavandi, S. Ahmadjo, R. Sandaroos, and M. A. Shamekhi, *Polyolefins J.* **1**, 25 (2014).
37. L. C. Simona, C. P. Williams, J. B. P. Soares, and R. F. de Souza, *J. Mol. Catal. A: Chem.* **165**, 55 (2001).
38. H. Arabi, M. S. Beheshti, M. Yousefi, N. Ghasemi Hamedani, and M. Ghafelebashi, *Polym. Bull.* **70**, 2765 (2013).
39. Zh. Guan and Ch. S. Popeney, *Top. Organomet. Chem.* **24**, 179 (2009).
40. M. Vatankhah-Varnoosfaderani, S. Pourmahdian, and F. Afshar-Taromi, *Iran. Polym. J.* **20**(11), 897 (2011).
41. S. P. Netalkar, S. Budagumpi, H. H. Abdallah, P. P. Netalkar, and K. Revankar, *J. Mol. Struct.* **1075**, 559 (2014).
42. G. H. Zohuri, R. Sandaroos, A. Mohammadi, S. M. Seyedi, and S. Damavandi, *Catal. Lett.* **140**, 160 (2010).
43. N. Bahri-Laleh, M. Nekoomanesh-Haghighi, and S. A. Mirmohammadi, *J. Organomet. Chem.* **719**, 74 (2012).